INTERNATIONAL JOURNAL FOR NUMERICAL METHODS IN FLUIDS
Int. J. Numer. Meth. Fluids 2002; **40**:79–91 (DOI: 10.1002/fld.268)

Local adaptive methods for convection dominated problems

Robert Klöfkorn*,†, Dietmar Kröner‡ and Mario Ohlberger§

Institut für Angewandte Mathematik, Universität Freiburg, Hermann-Herder-Str. 10, 79104 Freiburg, Germany

SUMMARY

In this paper, we consider rigorous *a posteriori* error estimates for convection dominated initial value problems including recent results for those with degenerating diffusion. These estimates are important to control the adaptive local mesh refinement for numerical computations, in particular for the simulation of the biodegradation process. Several results obtained by numerical experiments will be shown. Copyright © 2002 John Wiley & Sons, Ltd.

KEY WORDS: finite volume scheme; adaptive methods; *a posteriori* error estimates; biodegradation

1. INTRODUCTION

In order to compute numerical approximations of exact solutions of PDEs we want to minimize the computational costs in order to achieve a given tolerance, i.e. a given upper bound for the error between the exact and the numerical solution. One way to do this, is the method of local mesh refinement, which is controlled by the numerical solution itself on the basis of *a posteriori* error estimates. They measure the error between the exact and the numerical solution in terms of the numerical solution which is known. For elliptic and parabolic problems there exists a well developed theory which can be used to accelerate numerical codes considerably (see References [1–12]).

But if the PDEs are convection dominated with small diffusion, the constants in the *a posteriori* error estimates based on the L^2 theory can grow exponentially with decreasing diffusion. The situation will become even worse for pure convection problems, in particular for conservation laws. *A posteriori* error estimates in the $H^{-1,2}$-norm for the error and in the L^2-norm for the local error for linear symmetric hyperbolic systems have been shown in Reference [13]. In Reference [14] non-linear scalar conservation laws in ID have been considered. In that paper the author could estimate the error in the Lip′-norm, a special dual norm, by the residual.

*Correspondence to: R. Klöfkorn, Institut für Angewandte Mathematik, Universität Freiburg, Hermann-Herder-Strasse 10, 79104 Freiburg, Germany.
†E-mail: roberkt@mathematik.uni-freiburg.de
‡E-mail: dietmar@mathematik.uni-freiburg.de
§E-mail: mario@mathematik.uni-freiburg.de
URL: http://www.mathematik.uni-freiburg.de/IAM/

Received May 2001
Revised September 2001

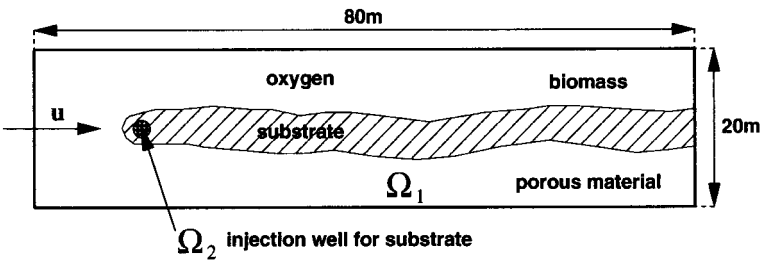

Figure 1. Schematic picture of the flow.

Just recently, we were able to prove a rigorous *a posteriori* error estimate for finite volume schemes on unstructured grids, discretizing the initial value problem for scalar conservation laws in multi-dimensions. Contrary to the elliptic case this estimate is based on the L^1-theory. The starting points for the proof are the Kruzkov entropy condition and the Kuznetsov [15] theory for getting local estimates. These *a posteriori* estimates take into account the finite propagation of perturbations of solutions for conservation laws. This means the local grid refinement is necessary only within the cone of dependence.

Closely related to this class of problems are convection diffusion problems with degenerate diffusion. The diffusion may degenerate on an open set, controlled by the solution itself if the diffusion is non-linear or by given diffusion coefficients. Also for this kind of PDEs *a posteriori* error estimates, which hold uniformly with respect to the diffusion, have been proved. The proof is mainly due to the concept of the generalization of entropy solutions to convection diffusion problems with degenerating diffusion.

A challenging problem for numerical approximations is the simulation of biodegradation [16] i.e. the transport and reaction of contaminants in porous media. We consider a channel filled with a porous medium (see Figure 1). Everywhere in the porous medium we have initially a small amount of biomass and, except in the well, oxygen. Initially we inject a substrate (e.g. oil) into the well. Then this substrate is transported by the underlying fluid with velocity u to the right part of the porous medium. The substrate will be degraded by a reaction between oxygen, substrate and biomass. The biomass will grow and the concentration of the substrate and oxygen will decrease. But the reaction will continue only in those regions where the concentration of the biomass, oxygen and substrate is large enough, this means mainly in the interface between the substrate and the surrounding region, where still enough oxygen is available. Within these interfaces, the concentration of the oxygen will rapidly decrease, such that here the biomass will die out. We expect that there is a sharp interface between the region of oxygen and that of the substrate (see Reference [16]). Now, if we use a numerical scheme with much numerical viscosity the interface between the substrate and oxygen is smeared out. Therefore, the reaction between the substrate and oxygen will take place in this smeared out region which is too large. This implies that the degradation of the substrate is too fast and we would get a completely wrong solution. In Plate 1 we see the result for a first-order finite volume scheme on a coarse grid. The substrate has been degraded to zero too early. Plate 2 shows the biomass at that time.

For the used data we expect (see Reference [16]) that for $T = 180$ days there is still a long, thin layer of the substrate up to the right boundary of the channel. Therefore in this case it

is absolutely necessary to get a high resolution of the transient region between the substrate and the oxygen. In order to achieve this we have to use higher order schemes and a good *a posteriori* error estimator for local grid refinement in the transient region.

The mathematical model for the biodegradation consists of a weakly coupled system (1), (2), (3) for the concentrations c_o, c_s and X of the oxygen, the substrate and the biomass, respectively.

$$\phi\partial_t c_o + \operatorname{div}(uc_o - \phi D(u)\nabla c_o) = -v_o k_{gr}(c_o, c_s, X) \tag{1}$$

$$\phi\partial_t c_s + \operatorname{div}(uc_s - \phi D(u)\nabla c_s) = -v_s k_{gr}(c_o, c_s, X), \quad \text{in }]0,80[\times]0,20[\times]0,T[\tag{2}$$

$$\partial_t X = v_X k_{gr}(c_o, c_s, X) - k_{dec} X. \tag{3}$$

Here, the transport of the oxygen and the substrate are linear and are given by the known velocity u. The porosity $\phi \in [0,1]$ is a given constant. The diffusion $D : \mathbb{R}^d \times \mathbb{R} \to \mathbb{R}^{d\times d}$ is assumed to be a non-linear tensor of x and u which can degenerate. The reaction rates are assumed to be of the form

$$k_{gr}(c_o, c_s, X) := \mu \frac{c_o}{c_o + K_o} \frac{c_s}{c_s + K_s} X. \tag{4}$$

The constant v_o, v_s and v_X denote the corresponding stoichiometric coefficients and k_{dec} the rate of decay of the biomass X. For the biomass we assume that there is no transport and no diffusion. The initial and boundary conditions will be specified in Section 4.

We want to derive an *a posteriori* error estimate for this weakly coupled system in order to reduce the numerical viscosity in the critical transient region. The most challenging point is that the diffusion may degenerate and that the *a posteriori* estimate should hold uniformly with respect to the lower bound of $D(x,u)$.

In order to demonstrate the main problems, let us consider the simple initial boundary value problem

$$\begin{aligned} \partial_t u + \operatorname{div} f(u) - \varepsilon\Delta u &= f && \text{in } \Omega_T \\ u &= 0 && \text{on } \partial\Omega\times]0,T[\\ u(x,0) &= u_0(x) && \text{on } \Omega \end{aligned} \tag{5}$$

with the small diffusion parameter ε. General energy based techniques for getting *a priori* error estimates give the following result (see Reference [17]).

Theorem 1 ([17])
Let u denote the exact solution of (5) and u_h the corresponding numerical solution obtained by a mixed finite volume finite element method (see (28) and (29)) and h the grid size. Then we have

$$\|u(\cdot,t^k) - u_h(\cdot,t^k)\|_{L^2(\Omega)} \leqslant ch^\alpha e^{cT/\varepsilon}, \tag{6}$$

where α and c are positive constants.

This estimate strongly depends on the small parameter ε and will explode if ε tends to zero. The situation is similar for the boundary value problem (7) and (8).

$$-\varepsilon\Delta u + a \cdot \nabla u + bu = f \quad \text{in } \Omega, \tag{7}$$

$$u = 0 \quad \text{on } \partial\Omega. \tag{8}$$

In Reference [18] for this problem the following *a posteriori* error estimate was proved. In this case u_h is given by a linear finite element method.

Theorem 2 ([18])

$$\|u - u_h\|^2 \leqslant \sum_{T \in \mathscr{T}_\ell} \eta_T^2 + \cdots (\text{data approximations}) \cdots \tag{9}$$

where

$$\eta_T := \min\left\{\frac{h}{\sqrt{\varepsilon}}, 1\right\} \|f_h - Lu_h\|_{L^2(T)} + \cdots \tag{10}$$

The estimate is uniform only if the grid size h is of the order of the parameter ε. There are some results mainly in 1D where similar estimates have been proved, uniformly in ε [7, 19]. While in References [18, 17] and many other papers the estimates are based on L^2 energy methods, in this paper we will give an overview of recent results concerning *a posteriori* error estimates, which are based on the Kuznetsov method [15]. It was developed for the pure non-linear hyperbolic case and can be generalized to the following equation (see Reference [20]).

$$\partial_t u + \operatorname{div}(vf(u) - D(u)\nabla u) + \lambda(u) = 0 \quad \text{in } \mathbb{R}^d \times]0, T[, \tag{11}$$

$$u(\cdot, 0) = u_0 \quad \text{in } \mathbb{R}^d \tag{12}$$

where the diffusion $D(u)$ may degenerate. Here λ is a given non-linear source term.

In the following, Section 2 we will briefly describe a finite volume scheme for solving scalar non-linear conservation laws in multi-dimension. Then we present *a posteriori* error estimates for this scheme. In Section 3 we will discuss some corresponding results for the initially value problem for (11) and (12). Finally in Section 4 recent results concerning numerical experiments for (1), (2) and (3) will be shown.

2. *A POSTERIORI* ERROR ESTIMATES FOR CONSERVATION LAWS

In this section, we are going to discuss an *a posteriori* error estimate [21] for

$$\partial_t u + \operatorname{div} f(u) = 0 \quad \text{in } \mathbb{R}^d \times \mathbb{R}^+, \tag{13}$$

$$u(x, 0) = u_0(x) \quad \text{in } \mathbb{R}^d. \tag{14}$$

For the data we have to assume the following conditions. $u_0 \in L^\infty(\mathbb{R}^d) \cap BV_{\text{loc}}(\mathbb{R}^d)$ with constants A and B such that $A \leqslant u_0 \leqslant B$ a.e. and $f \in C^1(\mathbb{R})$.

Let $\mathscr{T} = \{T_j \mid j \in I\}$ be a mesh of $\mathbb{R}^d$ such that the interface of two neighbouring cells T_j, T_l of $\mathscr{T}$ is included in a hyperplane (see also Reference [21]). The joint edge of T_j and T_l will be denoted by S_{jl}. We assume that, for all $h>0$, there exists an $\alpha>0$ such we have

$$\alpha h^d \leqslant \text{meas}(T_j), \quad \alpha\,\text{meas}(S_{jl}) \leqslant h^{d-1}, \quad \text{diam}(T_j) \leqslant h \tag{15}$$

for all $j, l \in I$. For any $j, l \in I$ there is a numerical flux $g_{jl} : \mathbb{R}^2 \to \mathbb{R}$ which satisfies the following conditions for all $u, v, u', v' \in [A, B]$.

$$\begin{aligned}&\text{The numerical flux } g_{jl}(u,v) \text{ is monotone increasing with}\\ &\text{respect to } u \text{ and monotone decreasing with respect to } v\end{aligned} \tag{16}$$

Furthermore

$$g_{jl}(u,v) = -g_{lj}(v,u), \quad g_{jl}(u,u) = n_{jl}|S_{jl}|f(u), \tag{17}$$

$$|g_{jl}(u,v) - g_{jl}(u',v')| \leqslant L h_{jl}(|u-u'| + |v-v'|) \tag{18}$$

where $h_{jl} := \max\{\text{diam}\, T_j, \text{diam}\, T_l\}$, Δt is the timestep, $t^n := n\Delta t$ and n_{jl} is the outer unit normal to S_{jl}. Now the upwind finite volume scheme for computing approximate solutions to (13) and (14) is defined by

Definition 1 (*Finite volume scheme*)
Let

$$u_j^0 := \frac{1}{|T_j|}\int_{T_j} u_0, \quad u_j^{n+1} := u_j^n - \frac{\Delta t}{|T_j|}\sum_{l \in N(j)} g_{jl}(u_j^n, u_l^n) \tag{19}$$

for all $n \in \mathbb{N}$ and $j, l \in I$. Here $N(j)$ denotes the indices of the neighbouring triangles of T_j.

For the time step we assume the following CFL-condition $\Delta t \leqslant (1-\xi)\alpha^2 h/2L$ for a given $\xi \in]0,1[$ and α as defined in (15), where L is the Lipschitz constant from (18). Let us denote

$$u_h(x,t) := u_j^n \quad \text{if } x \in T_j, \quad t^n < t \leqslant t^{n+1}. \tag{20}$$

Let u be the exact solution of (13) and (14) and u_h be the discrete solution as defined in (20). In Reference [22–24] it was shown that under the assumption, mentioned above, we have for any compact set $K \subset \mathbb{R}^d \times \mathbb{R}^+$

$$\int_K |u(x,t) - u_h(x,t)|\,\mathrm{d}x\,\mathrm{d}t \leqslant c h^{1/4} \tag{21}$$

where the constant c depends only on K and the given data.

Now let us present the corresponding *a posteriori* error estimate in the case $d=2$. Let R, ω, T be given and

$$\begin{aligned} I_0 &:= \left\{ n \mid 0 \leqslant t^n \leqslant \min\left\{\frac{R+1}{\omega}, T\right\}\right\}\\ D_{R+1} &:= \{(x,t) \mid |x - x_0| + \omega t < R+1\}\\ M(t) &:= \{j \mid \text{there exists } x \in T_j \text{ such that } (x,t) \in D_{R+1}\}. \end{aligned} \tag{22}$$

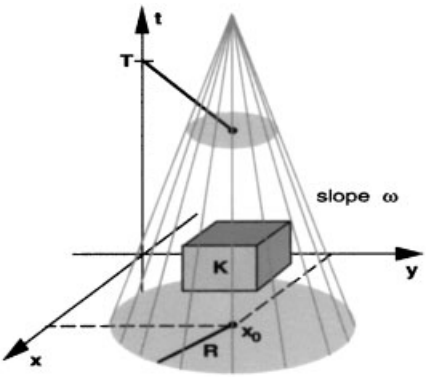

Figure 2. Cone of dependence.

Theorem 3 ([21])
Assume the conditions as mentioned above and $u_0 \in BV(\mathbb{R}^2)$. Let $K \subset\subset \mathbb{R}^2 \times \mathbb{R}^+, \omega = \sup_{A \leqslant s \leqslant B} |f(s)|$ and choose T, R and x_0 such that $T \in]0, R/\omega[$ and see Figure 2)

$$K \subset \bigcup_{0 \leqslant t \leqslant T} B_{R-\omega t}(x_0) \times \{t\}. \tag{23}$$

Then we have

$$\int_K |u - u_h| \leqslant T a_0 \left(\int_{|x-x_0|<R+1} |u_0(x) - u_h(x,0)| \, \mathrm{d}x + aQ + 2\sqrt{bcQ} \right) \tag{24}$$

where

$$Q := \sum_{n \in I_0} \sum_{j \in M(t^n)} \Delta t^n h_j^2 |u_j^{n+1} - u_j^n| + 2L\Delta t^n \sum_n \sum_{E(t_n)} (\Delta t + h_{jl}) h_{jl} |u_j^n - u_l^n| \tag{25}$$

and $E(t_n)$ is the set of all edges, which lie in $M(t^n)$. In the sum over $E(t_n)$ the indices j, l refer to the triangles T_j, T_l such that $T_j \cap T_l$ is the corresponding edge.

Remark 4
The constants a_0, a, b, c are explicitly known. A corresponding result also holds in $\mathbb{R}^d$ with $d > 2$. Under suitable conditions this theorem can be generalized if we replace $f(u)$ by $f(x,t,u)$ (see Reference [21]).

Example 5
Now let us use the *a posteriori* error estimate of Theorem 3 for the following numerical experiment. We want to solve (13) and (14) with $f(u) := (u^2, u^2)^t$ and

$$u_0(x) = 2 \quad \text{if } \frac{x_1 + x_2}{2} - 0.5 \leqslant 0,$$
$$u_0(x) = 1 \quad \text{if } \frac{x_1 + x_2}{2} - 0.5 > 0.$$

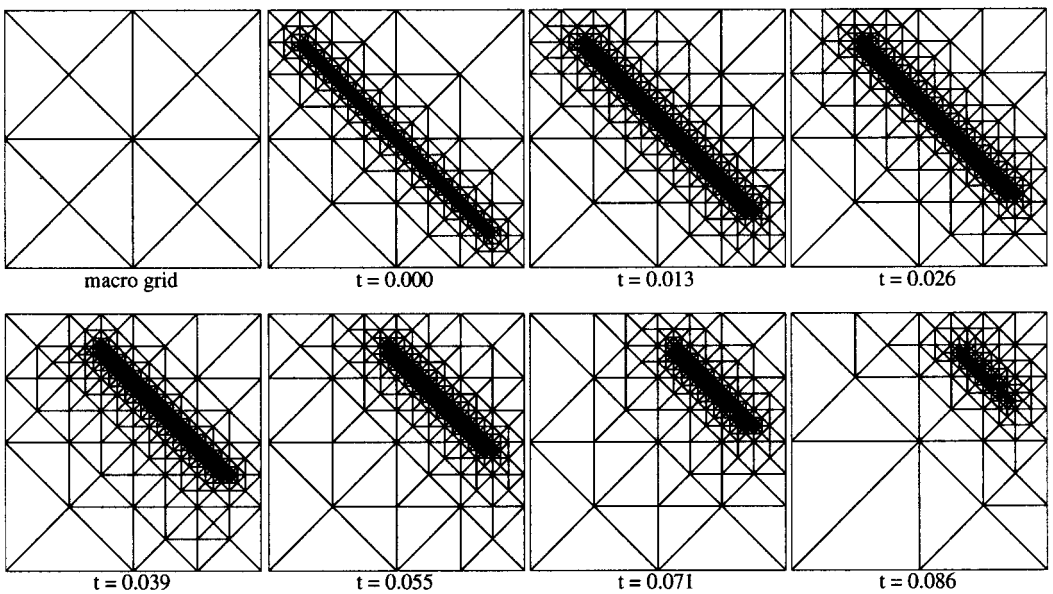

Figure 3. Burgers shocktype problem.

We want to get an approximate solution such that the error measured in the L^1-norm at time $t = 0.086$ in the circle $B_{0.1}(0.75, 0.75)$ is within a given tolerance. The corresponding grids which are produced by the error estimator of Theorem 3 for different times can be seen in Figure 3.

3. *A POSTERIORI* ERROR ESTIMATES FOR CONVECTION DOMINATED DIFFUSION EQUATIONS

The result in Theorem 3 can be generalized to the following convection dominated diffusion equation.

$$\partial_t u + \operatorname{div}(v f(u) - D(u)\nabla u) + \lambda u = 0 \quad \text{in } \mathbb{R}^d \times]0, T[, \tag{26}$$

$$u(\cdot, 0) = u_0 \quad \text{in } \mathbb{R}^d. \tag{27}$$

For the data we assume that

$$f \in C^2(\mathbb{R}, \mathbb{R}), \text{ and all derivatives are bounded, } D \in C^1(\mathbb{R}), \; D(s) > 0 \; \forall s \in \mathbb{R},$$

$$v \in (C^1 \cap L^\infty)(\mathbb{R}^d \times]0, T[, \mathbb{R}^2), \quad \operatorname{div} v = 0,$$

$$\lambda \in (C^1 \cap L^\infty)(\mathbb{R}^d \times]0, T[, \mathbb{R}), \quad u_0 \in (L^\infty \cap W^{1,1})(\mathbb{R}^d, \mathbb{R}).$$

Now since $D(u)$ can degenerate, it turns out that weak solutions in $L^1(\mathbb{R}^d \times \mathbb{R}^+)$ are not unique. Therefore we have to define entropy solutions, similar as for conservation laws.

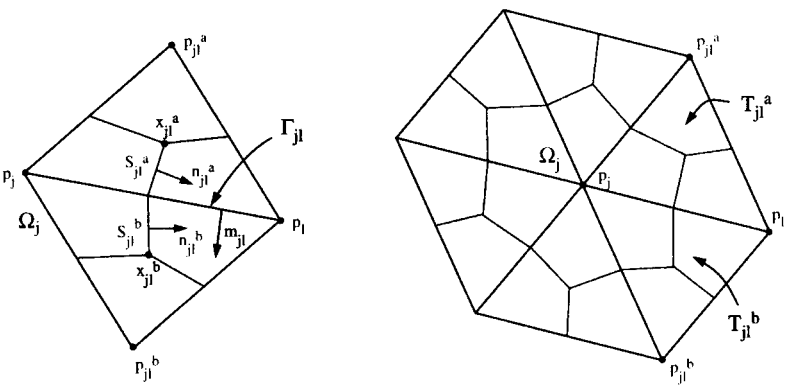

Figure 4. Notation of the triangulation and dual mesh.

Definition 2 (*Entropy solution*)
Let U be a smooth, strict convex entropy function and F a corresponding entropy flux ($\partial_v F(v,\kappa) = f'(v)U'(v-\kappa)$). A weak solution of (26) and (27) is called an entropy solution of (26) and (27) if,

$$\int_{\mathbb{R}^d\times\mathbb{R}^+} U(u-\kappa)\partial_t\varphi + [F(u,\kappa)v - D(u)U'(u-\kappa)\nabla u]\cdot\nabla\varphi - \lambda CU'(u-\kappa)\varphi$$
$$+\int_{\mathbb{R}^d} U(u_0-\kappa)\varphi(\cdot,0) \geqslant \int_{D(u(x,t))>0} D(u)U''(u-\kappa)|\nabla u|^2\varphi$$

$\forall\varphi\in C_0^\infty(\mathbb{R}^d\times[0,T[),\ \forall\varphi\geqslant 0,\ \forall\kappa\in\mathbb{R}$.

It was shown in Reference [25] that under the above assumptions a unique entropy solution u of (26) and (27) exists. Now let us describe the numerical scheme for which we will show an *a posteriori* result. The scheme is similar to that one in Reference [17]. The notation will be explained in Figure 4. The triangulation has to satisfy the conditions (15), and the numerical fluxes the conditions (16), (17), (18) mentioned in Section 2. Let

$$u_j^0 := \frac{1}{|\Omega_j|}\int_{\Omega_j} u_0, \tag{28}$$

$$u_j^{n+1} := u_j^n - \frac{\Delta t^n}{|\Omega_j|}\sum_{l\in N_j}\sum_{i\in\{a,b\}}[g_{jl}^{i,n+1}(u_{jl}^{n+1},u_l^{n+1}) - d_{jl}^{i,n+1}(u_h^{n+1})]$$
$$-\Delta t^n\lambda_j^{n+1}u_j^{n+1}. \tag{29}$$

Here u_h^n denotes the piecewise linear function which satisfies $u_h^n(p_j) = u_j^n$, and $d_{jl}^{i,n}(u_h) = \int_{S_{jl}^i} D\nabla u_h^n\cdot n_{jl}^i$. The following result has been proved in Reference [20].

Plate 1. Distribution of substrate after $T = 180$ days.

Plate 2. Distribution of biomass after $T = 180$ days.

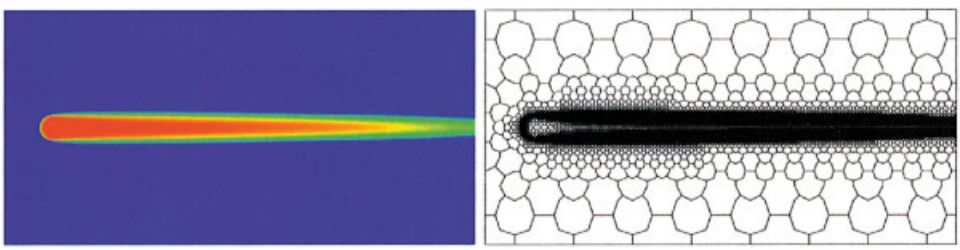

Plate 3. Reference solution on a fine adapted grid with 92837 dual cells.

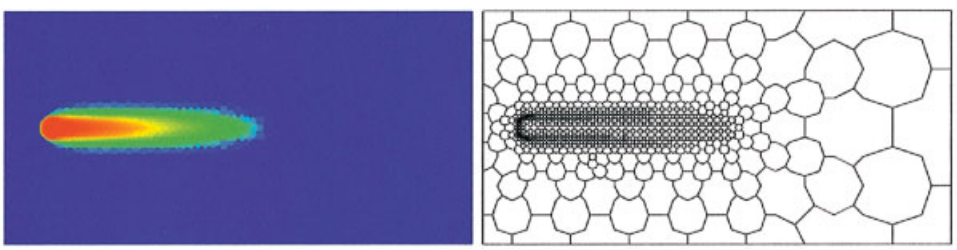

Plate 4. Example 9 with 1778 dual cells.

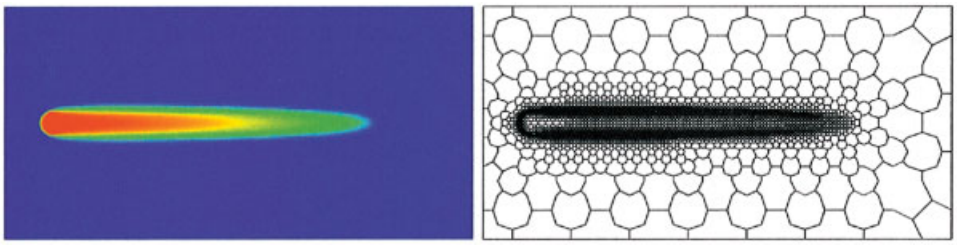

Plate 5. Example 9 with 10152 dual cells.

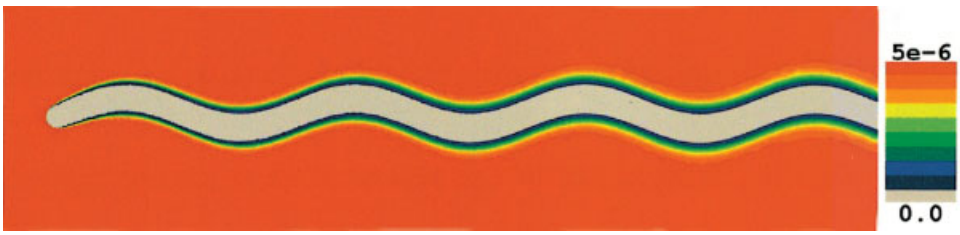

Plate 6. Distribution of oxygen after $T = 180$ days.

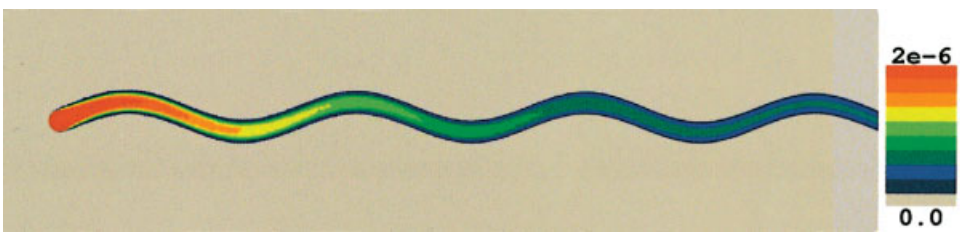

Plate 7. Distribution of substrate after $T = 180$ days.

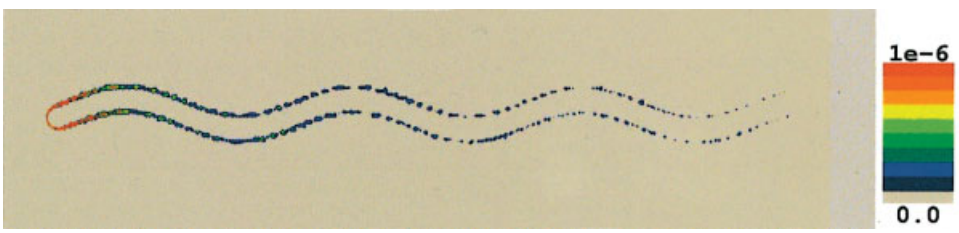

Plate 8. Distribution of biomass after $T = 180$ days.

Theorem 6 ([20])
Assume $D = \text{constant} > 0$, $\lambda = 0$. Then

$$\|u_h - u\|_{L^1(\mathbb{R}^d \times]0,T[)} \leqslant \eta$$

where

$$\eta := \frac{T}{\ln 2}(\eta_0 + k_2\tilde{\eta} + \sqrt{k_4\eta_u} + \sqrt{6k_3\tilde{\eta}}) \tag{30}$$

$$\tilde{\eta} := \eta_t + \eta_c + \eta_d + \eta_{p,1} \tag{31}$$

$$\eta_0 := \int_{\mathbb{R}^2} |u_h(x,0) - u_0(x)| \mathrm{d}x \tag{32}$$

$$\eta_t := \sum_n \sum_j |u_j^{n+1} - u_j^n| \Delta t^n |\Omega_j| \tag{33}$$

$$\eta_c := \sum_n \sum_{\text{dual edges}} (h_{jl} + \Delta t^n)\Delta t^n Q_{jl}^{i,n+1} |u_j^{n+1} - u_l^{n+1}| \tag{34}$$

$$\eta_d := \sum_n \sum_{\text{edges}} (h_{jl} + \Delta t^n)\Delta t^n |\Gamma_{jl}| D[\nabla u_h^{n+1} \cdot m_{jl}]_{\Gamma_{jl}} \tag{35}$$

$$\eta_u := 4 \sum_n \sum_{\text{edges}} D[\nabla u_h^{n+1} \cdot m_{jl}]_{\Gamma_{jl}} \Delta t^n |\Gamma_{jl}| |u_j^{n+1} - u_l^{n+1}| \tag{36}$$

$$\eta_{p,1} := \sum_n \sum_j (1 + |v|L_f) h_j \Delta t^n \int_{\Omega_j} |\nabla u_h(x, t^{n+1})| \mathrm{d}x \tag{37}$$

$$Q_{jl}^{n+1}(v,w) := \frac{2g_{jl}^{i,n+1}(v,w) - g_{jl}^{i,n+1}(v,v) - g_{jl}^{i,n+1}(w,w)}{(v-w)} \tag{38}$$

$$[\nabla u_h^{n+1} \cdot m_{jl}]_{\Gamma_{jl}} := |(\nabla u_h^{n+1}|_{T_{jl}^s} - \nabla u_h^{n+1}|_{T_{jl}^b}) \cdot m_{jl}|. \tag{39}$$

$\sum_n$ denotes the sum over all timesteps, $\sum_{\text{dual edges}}$ the sum over all edges of the dual cells. If S_{jl}^i is a dual edge, then j and l are defined as in Figure 4. $\sum_{\text{edges}}$ denotes the sum over all edges of the triangles. If Γ_{jl} is one of these edges, then j, l are defined again by Figure 4. All constants are known explicitly.

Remark 7
If $\lambda \neq 0$ a similar result holds with a modified η depending on λ.

Remark 8
In a forthcoming paper [26] this result will be generalized to weakly coupled systems as in Reference [27]. Then the mathematical model for the biodegradation (1), (2) and (3) will be covered by this generalization.

Example 9
Now again let us use the *a posteriori* error estimate of Theorem 6 for the following numerical experiment (for details see Reference [20]). We want to solve

$$\begin{aligned} \phi\partial_t u + \operatorname{div}(vf(u) - KD\nabla u) + \lambda(\cdot,u) = 0 \quad & \text{in }]0,1[\times]0,0.5[\times]0,T[, \\ u(\cdot,0) = 1 \quad & \text{in } B_{0,0.25}(0.1,0.25), \\ u(\cdot,0) = 0 \quad & \text{else} \end{aligned}$$

where

$$f(u) := u^2, \quad v = (0.5, 0), \quad D = 0.0001, \quad \phi = 0.2, \quad K = 0.2$$

and

$$\begin{aligned} \lambda(\cdot,u) &= 10u(1-u)^3 - 100\,\frac{1-u}{1-u+0.1} \quad \text{in } B_{0.025}(0.1,0.25), \\ \lambda(\cdot,u) &= 10u(1-u)^3 \text{ else.} \end{aligned}$$

The reference solution on a very fine adapted grid can be seen in Plate 3. The results in Plates 4 and 5 indicate that for grids with less resolution the length of the contaminated area is too short.

4. NUMERICAL EXPERIMENTS FOR BIODEGRADATION

In this section, we will present some numerical results concerning the system (1), (2) and (3). This is a mathematical model for the process of biodegradation. In this case, we use the definition (4) and

$$\begin{gathered} \phi = 0.3, \;\; u(x,t) = \left(2\times10^{-5}, 8\times10^{-6}\,\sin\left(\frac{6}{80}\,x_1 - \frac{1}{20}\right)\right)^{\mathrm{t}}, \\ D(u)_{ij} := \varepsilon\delta_{ij} + \alpha_T\delta_{ij}|u| + (\alpha_L - \alpha_T)\frac{u_i u_j}{|u|}, \\ \varepsilon = 10^{-9}, \;\; \alpha_T = 0.002, \;\; \alpha_L = 0.01 \end{gathered}$$

and $K_o, K_s, v_o, v_s, k_{dec}, \mu$ are suitable constants (see Reference [16]). We consider the following initial values for (1), (2) and (3)

$$\begin{aligned} c_o(x,0) &= 5\times10^{-6} \quad \text{in } \Omega_1 \\ c_o(x,0) &= 0 \quad \text{in } \Omega_2 \\ c_s(x,0) &= 0 \quad \text{in } \Omega_1 \\ c_s(x,0) &= 2\times10^{-6} \quad \text{in } \Omega_2 \\ X(x,0) &= 10^{-9} \quad \text{in } \Omega_1 \cup \Omega_2. \end{aligned} \tag{40}$$

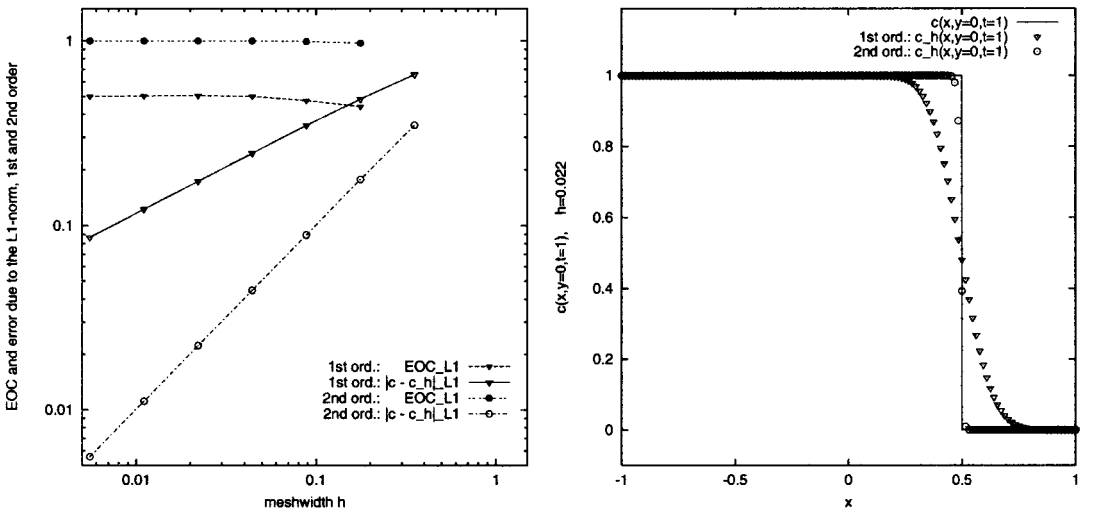

Figure 5. EOC and numerical solutions.

Table I. EOC_{L^1} and L^1-error for the finite volume scheme first [A] and second [B] order.

h	$\|c - c_h^A\|_{L^1}$	$\mathrm{EOC}^{\mathrm{A}}_{\mathrm{L}^1}$	$\|c - c_h^B\|_{L^1}$	$\mathrm{EOC}^{\mathrm{B}}_{\mathrm{L}^1}$	CPU-time in s A vs B		Memory usage in MB	
0.3536	0.6579		0.3485		0.1	0.1	0.1	0.1
0.1768	0.4847	0.441	0.1776	0.973	0.2	0.9	0.2	0.2
0.0884	0.3485	0.476	0.0892	0.993	3	7	0.6	0.6
0.0442	0.2462	0.502	0.0446	0.999	28	57	2.3	2.4
0.0221	0.1735	0.505	0.0223	1.0	235	487	8.7	9.3
0.0110	0.1224	0.503	0.0112	1.0	1916	4016	34.4	36.9
0.0055	0.0865	0.501	0.0056	1.0	15528	33315	137.3	147.3

As boundary conditions we use

$$c_{\mathrm{o}} = 5 \times 10^{-6},\ c_{\mathrm{s}} = 2 \times 10^{-6} \text{ on the left, lower, and upper boundary of the channel.} \tag{41}$$

On the right part of the channel we need no conditions for $c_{\mathrm{o}}, c_{\mathrm{s}}$ since the x-component of the velocity u is positive and since we use an upwinding discretization. The discretization for (1), (2) and (3) is a mixed finite volume finite element method as described in (28) and (29) for the scalar equation. It is explicit for the convective terms and implicit for the diffusive terms. In addition to that we use a higher order discretization in space, based on non-linear limiters. For the validation of the scheme we have used a linear transport problem for which we know the exact solution. The error and the experimental order of convergence are shown in Figure 5 and Table I.

In Plates 6, 7 and 8 the numerical solutions for (1), (2), (3), (40), (41) obtained by (28), (29) are shown. For the *a posteriori* error estimate we use the indicators (32),...,(35) as

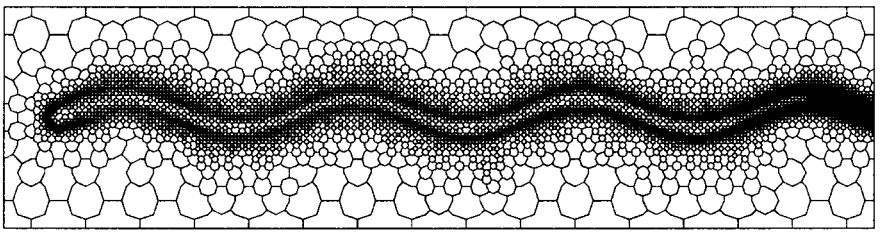

Figure 6. Adapted dual mesh with 7530 cells.

defined in Theorem 6 for each component. The sum of these is used in the definition of η in (30). We obtain a layer of the transported substrate up to the right boundary of the channel. The interfaces between the substrate and the oxygen in the neighbourhood remains sharp. This is consistent with the results in Reference [16] which are obtained on a fixed unstructured grid. In Figure 6 the corresponding locally refined grid, which is produced with the error estimator of Theorem 6, is presented.

REFERENCES

1. Angermann L, Knabner P, Thiele K. An error estimate for a finite volume discretization of density driven flow in porous media. *Applied Numerical Mathematics* 1998; **26**:179–191.
2. Becker R, Rannacher R. A feed-back approach to error control in finite element methods: basic analysis and examples. *East–West Journal on Numerical Mathematics* 1996; **4**:237–264.
3. Braess D, Verfürth R. *A posteriori* error estimators for the Raviart–Thomas element. *SIAM Journal on Numerical Analysis* 1996; **33**:2431–2444.
4. Dörfler W. A robust adaptive strategy for the nonlinear poisson equation. *Computing* 1995; **55**:289–304.
5. Dörfler W. A convergent adaptive algorithm for poisson's equation. *SIAM Journal on Numerical Analysis* 1996; **33**:1106–1124.
6. Dörfler W. A time- and spaceadaptive algorithm for the linear time-dependent Schrödinger equation. *Numerische Mathematik* 1996; **73**:419–448.
7. Dörfler W. *Uniformly Convergent Finite-Element Methods for Singularly Perturbed Convection-Diffusion Equations*. Habilitationsschrift, Mathematische Fakultät: Freiburg, 1998.
8. Eriksson K, Johnson C. Adaptive streamline diffusion finite element methods for stationary convection-diffusion problems. *Mathematics of Computation* 1993; **60**:167–188.
9. Eriksson K, Johnson C. Adaptive finite element methods for parabolic problems. V: Long-time integration. *SIAM Journal on Numerical Analysis* 1995; **32**:1750–1763.
10. Houston P, Süli E. Adaptive Lagrange–Galerkin methods for unsteady convection-dominated diffusion problems. *Report 95/24*, Numerical Analysis Group, Oxford University Computing Laboratory, 1995.
11. Claes Johnson, Rolf Rannacher, Mats Boman. Numerics and hydrodynamic stability: toward error control in computational fluid dynamics. *SIAM Journal on Numerical Analysis* 1995; **32**(4):1058–1079.
12. Rannacher R. Hydrodynamic stability and *a posteriori* error control in the solution of the Navier–Stokes equations. In *Calculus of Variations*, *Applications and Computations* (*Pont-à-Mousson*, *1994*), Longman Sci. Tech., Harlow 1995; 188–200.
13. Houston P, Mackenzie JA, Süli E, Warnecke G. *A posteriori* error analysis for numerical approximation of Fridrichs system. *Numerische Mathematik* 1999; **82**(3):433–470.
14. Tadmor E. Local error estimates for discontinuous solutions of nonlinear hyperbolic equations. *SIAM Journal on Numerical Analysis* 1991; **28**:891–906.
15. Kuznetsov NN. Accuracy of some approximate methods for computing the weak solutions of a first-order quasi-linear equation. *USSR*, *Computational Mathematics*, *Mathematical Physics* 1976; **16**(6):159–193.
16. Cirpka O, Frind E, Helmig R. Numerical simulation of biodegradation controlled by transverse mixing. *Journal of Contaminant Hydrology* 1999; **40**:159–182.
17. Feistauer M, Felcman J, Lukáčová-Medvid'ová M. On the convergence of a combined finite volume–finite element method for nonlinear convection-diffusion problems. *Numerical Methods for Partial Differential Equations* 1997; **13**:163–190.

18. Verfürth R. Robust *a posteriori* error estimators for a singularly perturbed reaction-diffusion equation. *Numerische Mathematik* 1998; **78**:479–493.
19. Johnson C, Szepessy A. Adaptive finite element methods for conservation laws based on *a posteriori* error estimates. *Communications on Pure and Applied Mathematics* 1995; **48**:199–234.
20. Ohlberger M. *A posteriori* error estimates for vertex centered finite volume approximations of convection-diffusion-reaction equations. *M2AN Mathematical modelling and Numerical Analysis* 2001; **35**(2):355–387.
21. Kröner D, Ohlberger M. *A posteriori* error estimates for upwind finite volume schemes for nonlinear conservation laws in multidimensions. *Mathematics of Computation* 2000; **69**:25–39.
22. Chainais-Hillairet C. Finite volume schemes for a nonlinear hyperbolic equation. Convergence towards the entropy solution and error estimates. *M2AN Mathematical modelling and Numerical Analysis* 1999; **33**:129–156.
23. Vila JP. Convergence and error estimates in finite volume schemes for general multi-dimensional scalar conservation laws. I Explicit monotone schemes. *RAIRO*, *Modelisation Mathematique et Analyse Numerique* 1994; **28**:267–295.
24. Cockburn B, Coquel F, Lefloch PG. An error estimate for finite volume methods for multidimensional conservation laws. *Mathematics of Computation* 1994; **63**:77–103.
25. Carrillo J. Entropy solutions for nonlinear degenerate problems. *Archive for Rational Mechanics and Analysis* 1999; **147**:269–361.
26. Ohlberger M, Rohde C. Adaptive finite volume approximations for weakly coupled convection dominated parabolic systems. *IMA Journal of Numerical Analysis* 2002; **22**:253–280.
27. Christian Rohde. Entropy solutions for weakly coupled hyperbolic systems in several space dimensions. *Zeitschrift Fur Angewandte Mathematik und Physik* 1998; **49**(3):470–499.

